



**HAL**  
open science

# Bifunctional Hexadentate Pyclyen–Based Chelating Agent for Mild Radiofluorination in Aqueous Solution at Room Temperature with a Ga- 18 F Ternary Complex

Fabienne Dioury, Carine San, Gayathiri Gnanalingam, Céline Henoumont, Yoann Rousselin, Ahmed Haouz, William Shepard, Benoît Hosten, Kamsana Vijayakumar, Sophie Laurent, et al.

## ► To cite this version:

Fabienne Dioury, Carine San, Gayathiri Gnanalingam, Céline Henoumont, Yoann Rousselin, et al.. Bifunctional Hexadentate Pyclyen–Based Chelating Agent for Mild Radiofluorination in Aqueous Solution at Room Temperature with a Ga- 18 F Ternary Complex. *Chemistry - A European Journal*, 2024, 30 (68), pp.e202403358. 10.1002/chem.202403358 . hal-04826589

**HAL Id: hal-04826589**

**<https://hal.science/hal-04826589v1>**

Submitted on 9 Dec 2024

**HAL** is a multi-disciplinary open access archive for the deposit and dissemination of scientific research documents, whether they are published or not. The documents may come from teaching and research institutions in France or abroad, or from public or private research centers.

L'archive ouverte pluridisciplinaire **HAL**, est destinée au dépôt et à la diffusion de documents scientifiques de niveau recherche, publiés ou non, émanant des établissements d'enseignement et de recherche français ou étrangers, des laboratoires publics ou privés.



Distributed under a Creative Commons Attribution - NonCommercial - NoDerivatives 4.0 International License

# Bifunctional Hexadentate PycLen–Based Chelating Agent for Mild Radiofluorination in Aqueous Solution at Room Temperature with a Ga-<sup>18</sup>F Ternary Complex

Fabienne Dioury,<sup>\*[a]</sup> Carine San,<sup>[a, b]</sup> Gayathiri Gnanalingam,<sup>[a]</sup> Céline Henoumont,<sup>[c]</sup> Yoann Rousselin,<sup>[d]</sup> Ahmed Haouz,<sup>[e]</sup> William Shepard,<sup>[f]</sup> Benoît Hosten,<sup>[b, g]</sup> Kamsana Vijayakumar,<sup>[a]</sup> Sophie Laurent,<sup>[c]</sup> and Marc Port<sup>\*[a]</sup>

Positron Emission Tomography (PET) is used in oncology for tumor diagnosis, commonly relying on fluorine-18 (<sup>18</sup>F) emission detection. The conventional method of <sup>18</sup>F incorporation on to probes by covalent bonding is harsh for sensitive biomolecules, which are nonetheless compounds of choice for the development of targeted probes. This study explores gallium-<sup>18</sup>F (Ga<sup>18</sup>F) coordination, a milder alternative method occurring in aqueous media at the final stage of radiosyntheses. PycLen-based chelating agents were proposed to capture (GaF) species at room temperature and  $pH \geq 5$  making the radiofluorination process compatible with heat- and acid-sensitive biomolecules. Highly promising results were obtained with the PC2A-based

chelating agent LH<sub>2</sub> derived from the new bifunctional PC2A–OAE–NCS compound. The solid-state structure of GaF(L) was elucidated by X-ray diffraction and revealed an unconventional heptacoordination of Ga(III). A high radiochemical conversion (RCC) of 86% was achieved at room temperature, in water at  $pH$  5 within 20 minutes. Stability studies showed the robustness of the GaF(L) complex in aqueous media for at least one day and at least one hour for the radiolabeled analog Ga<sup>18</sup>F(L). These findings demonstrated that PC2A-based compounds are chelating agents of choice for (Ga<sup>18</sup>F) species, suggesting a real technological breakthrough for PET imaging and precision medicine.

## Introduction

Positron Emission Tomography (PET) has emerged as a revolutionary medical imaging technique, offering deep insights into the functional aspects of tissues. It plays a major role in oncology for the diagnosis and initial evaluation of various types of tumors, and is also used in cardiology, neurodegenerative, inflammation, or infectious diseases.<sup>[1–4]</sup> PET is based on the detection of positrons, charged particles emitted by certain radioactive isotopes. Among these isotopes, fluorine-18 (<sup>18</sup>F) stands out as the most widely employed, owing to its unique physical properties. Its half-life ( $t_{1/2}$ ) of 110 min offers a good compromise: long enough for transport, eliminating the need for an on-site cyclotron, and short enough for a clinical imaging

procedure to be completed in less than 2 hours. Moreover, <sup>18</sup>F has an almost pure positron emission profile: 96.7% of  $\beta^+$  emission with 3.3% of electron capture followed by X-ray emissions whose energy and yield are low and do not penalize imaging or patient exposure. <sup>18</sup>F is also characterized by a low maximum  $\beta^+$  energy, ( $E_{\max}\beta^+ = 634$  keV). All these properties are in favor of improved sensitivity and resolution of the resulting images. Moreover, its production by cyclotrons and its half-life ensure a steady supply, large-scale production and distribution of radiotracers. Currently, commercial fluorine-labeled radiotracers such as [<sup>18</sup>F]fluorodeoxyglucose, [<sup>18</sup>F]fluorocholine, [<sup>18</sup>F]fluorodopa are synthesized using a conventional method based on nucleophilic substitution.

[a] F. Dioury, C. San, G. Gnanalingam, K. Vijayakumar, M. Port  
Conservatoire national des arts et métiers, Laboratoire Génomique,  
bioinformatique et chimie moléculaire (GBCM), EA 7528, 2 rue Conté, 75003  
Paris France  
E-mail: fabienne.dioury@lecnam.net  
marc.port@lecnam.net

[b] C. San, B. Hosten  
Hôpital Saint-Louis, Université Paris Cité, Institut de Recherche Saint-Louis,  
Unité Claude Kellershohn, 1 avenue Claude Vellefaux, 75010 Paris France

[c] C. Henoumont, S. Laurent  
Université de Mons, General, Organic and Biomedical Chemistry Group,  
NMR and Molecular Imaging Laboratory, Mendeleev building, 19 avenue  
Maistriau, B-7000 Mons Belgique

[d] Y. Rousselin  
Université de Bourgogne, Institut de Chimie Moléculaire de l'Université de  
Bourgogne (ICMUB), UMR CNRS 6302, 9 avenue Alain Savary, 21078 Dijon  
France

[e] A. Haouz  
Institut Pasteur, Crystallography Platform C2RT, CNRS UMR 3528, 25-28 rue  
du Docteur Roux, 75015 Paris, France

[f] W. Shepard  
Synchrotron SOLEIL, Proxima 2A, L'Orme des Merisiers, Départementale 128,  
91190 Saint-Aubin, France

[g] B. Hosten  
Université Paris Cité, INSERM UMR–S 1144, Optimisation Thérapeutique en  
Neuropsychopharmacologie, 4 avenue de l'Observatoire, 75006 Paris France

Supporting information for this article is available on the WWW under  
<https://doi.org/10.1002/chem.202403358>

© 2024 The Author(s). Chemistry - A European Journal published by Wiley-VCH GmbH. This is an open access article under the terms of the Creative Commons Attribution Non-Commercial NoDerivs License, which permits use and distribution in any medium, provided the original work is properly cited, the use is non-commercial and no modifications or adaptations are made.

This approach requires several steps, including  $^{18}\text{F}$  activation and a purification step, which lengthens the synthesis time, whereas the desirable time for the synthesis of  $^{18}\text{F}$ -labeled tracers and clinical use is less than a half-life, *i.e.* around 2 hours, in order to provide sufficient radioactivity for subsequent PET imaging of the patient, which can occur up to 6 half-lives after  $^{18}\text{F}$  production, *i.e.* 11 hours in the case of an  $^{18}\text{F}$  PET scan.<sup>[5]</sup> Additionally, it requires reaction conditions such as high temperature (up to  $110^\circ\text{C}$ ),  $^{18}\text{F}$  activation step (azeotropic drying), organic solvent, and/or catalysts, limiting the scope of application, for example to delicate biomolecules that can be denatured under these conditions. Meanwhile, the field of oncology continues to evolve, with immunotherapy and new personalized therapies taking center stage, so that demand for more specific imaging using biomolecules as targeting agents has surged. To address the need for a milder  $^{18}\text{F}$ -labeling methodology suitable for biomolecules, McBride *et al.* developed the aluminum- $^{18}\text{F}$  ( $\text{Al-}^{18}\text{F}$ ) species complexation method.<sup>[6]</sup> This  $\text{Al-}^{18}\text{F}$  complexation technology has emerged as a promising alternative for  $^{18}\text{F}$  PET tracer synthesis and this method has gained recognition and acceptance across numerous research teams as it relies on a bifunctional chelating agent previously conjugated to the probe which can trap the  $\text{Al}^{18}\text{F}$  generated *in situ* by mixing [ $^{18}\text{F}$ ]fluoride with aluminum trichloride.<sup>[7–9]</sup> When combined with macrocyclic NODA-based chelating agents, the  $\text{Al-}^{18}\text{F}$  complexation offers numerous advantages such as *in vivo* stability. However, a notable drawback of  $\text{Al-}^{18}\text{F}$  complexation technology is the need for high heating ( $110^\circ\text{C}$ ) and rather acidic conditions, with protocols typically performed at *pH* 4 to 4.5, thus limiting the strategy's compatibility with heat- and/or acid-sensitive biomolecules. To circumvent this limitation, acyclic chelating agents have been developed to trap  $\text{Al}^{18}\text{F}$  at a lower temperature ( $< 40^\circ\text{C}$ ),<sup>[10–12]</sup> but these promising systems still need to be refined before they can be applied to modified probes<sup>[11]</sup> and/or *in vivo* stability of the resulting radiotracers is still debated in the literature.<sup>[9]</sup> These recent results demonstrated that there is still room for the development of alternative radiolabeling methodology.

Like aluminum, gallium displays a strong affinity for the fluoride anion characterized by a high  $\text{Ga-F}$  bond dissociation

energy ( $584 \text{ kJ mol}^{-1}$  versus  $675 \text{ kJ mol}^{-1}$  for  $\text{Al-F}$ ),<sup>[13]</sup> allowing for the speculation of a similar radiofluorination process, *i.e.* by complexation of a pseudo-metallic ( $\text{Ga-}^{18}\text{F}$ ) species. Consequently, several chelating agents were developed and led to some  $\text{Ga-X}$  ( $\text{X} = \text{Cl}, \text{NO}_3, \text{F}$ ) preformed complexes that proved to be promising precursors for capturing the [ $^{18}\text{F}$ ] $\text{F}^-$  anion (Table 1). However, the results of these different studies are not fully satisfactory as the radiolabeling yields are rather low, or stringent reaction conditions cannot be circumvented, or the radiostability of the labeling has been poor, and research in the domain remains poorly described to date with, to our knowledge, in the current decade, only six articles referring to research on the technology ( $\text{Ga-}^{18}\text{F}$ ) (Table 1).<sup>[14–19]</sup>

Altogether, these reported studies suggest that  $\text{Ga}^{18}\text{F}$  complexation technology is of interest for biomolecule radiolabeling, but thorough exploration is required to optimize chelating agent structure and radiosynthesis conditions. Indeed, the use of  $\text{Ga}^{18}\text{F}$  has not yet led to the ideal mild aqueous one-step  $^{18}\text{F}$  labeling with high radiolabeling yield and radiostability.

To overcome these obstacles and make  $\text{Ga-}^{18}\text{F}$  technology effective for radiolabeling sensitive biomolecules, we have, in this work, designed and synthesized a novel bifunctional dianionic chelating agent  $\text{H}_2(\text{PC2A-OAE-NCS})$  (Figure 1) and used its derivative, denoted  $\text{LH}_2$ , to study the formation and characterization in cold chemistry of  $\text{Ga}^{19}\text{F}$  complexes. Ultimately, we studied the radiolabeling under mild conditions (room temperature) of  $\text{LH}_2$  and evaluated the radiostability of the  $\text{Ga}^{18}\text{F}(\text{L})$  complex obtained.

## Results and Discussion

### Design of $\text{GaF}(\text{L})$

Previous results from us and other groups showed that chelating agents derived from the trianionic chelating agent  $\text{H}_3(\text{PCTA})$  (Figure 1) strongly capture  $\text{Ga}(\text{III})$  species with fast kinetics at room temperature, in pure water.<sup>[20,21]</sup> In addition, unpublished preliminary results from our group on the solid-state X-ray structure of the  $\text{Ga}^{3+}$  complex formed with the

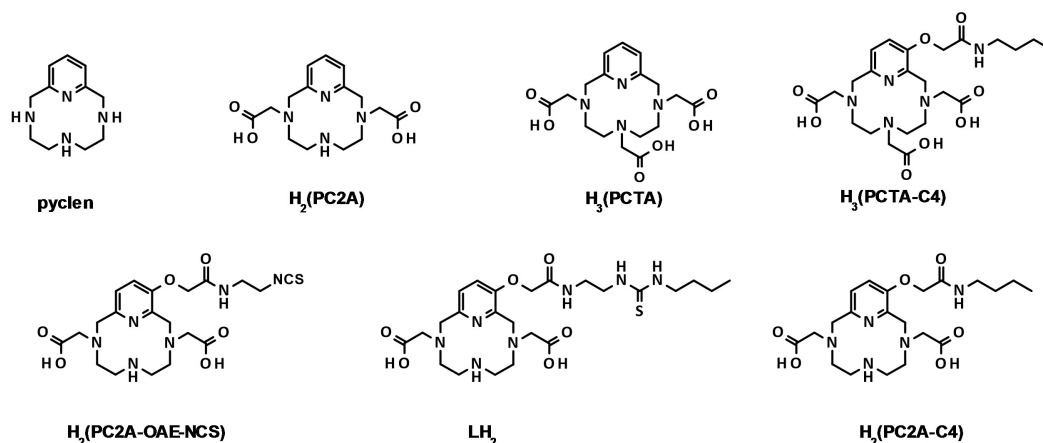


Figure 1. Compounds of pyclen backbone discussed herein.

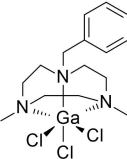
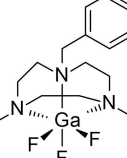
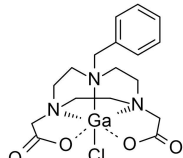
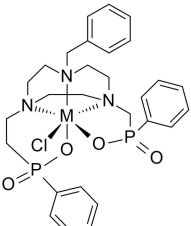
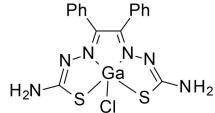
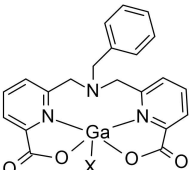
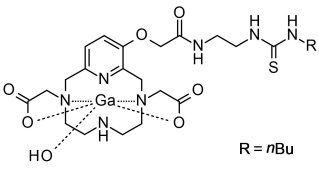
Entry	Precursor	Reaction conditions	RCY <sup>[a]</sup>	Stability (RCP) <sup>[b]</sup>	Ref
1	<b>GaCl<sub>3</sub>(BnMe<sub>2</sub>-tacn)</b> 	MeCN/H <sub>2</sub> O 50/50, r.t., 30 min <i>pH</i> not available	30 %	At least 2 hours in 10 % EtOH/PBS <i>pH</i> 7.5 (99 %)	[16]
2	<b>Ga<sup>19</sup>F<sub>3</sub>(BnMe<sub>2</sub>-tacn)</b> 	MeCN/H <sub>2</sub> O 8/92, r.t., 45 min MeCN/H <sub>2</sub> O 75/25, 80 °C, 10 min EtOH/H <sub>2</sub> O 75/25, 80 °C, 10 min <i>pH</i> not available	4 % 73 % 81 %	≤ 2 hours in 20 % EtOH/H <sub>2</sub> O (88 %) ≤ 2 hours in 10 % EtOH/HSA (83 %) ≤ 2 hours in 10 % EtOH/PBS <i>pH</i> 7.4 (74 %)	[17]
3	<b>GaCl(Bn-NODA)</b> 	AcONa/H buffer ( <i>pH</i> 4.0), 80 °C, 30 min AcONa/H buffer ( <i>pH</i> 4.0), r.t., 30 min	65–70 % 30 %	At least 4 hours in 10 % EtOH/NaOAc <i>pH</i> 4 At least 3 hours in 10 % EtOH/NaOAc <i>pH</i> 5 ≤ 20 minutes in 10 % EtOH/PBS <i>pH</i> 7.5 ≤ 20 minutes in HSA	[14]
4	<b>GaCl(Bn-NODP)</b> 	AcONa/H buffer/MeCN/H <sub>2</sub> O 45/30/25 80 °C, 10 min <i>pH</i> not available	71 %	At least 3.5 hours in 10 % EtOH/H <sub>2</sub> O (94 %) At least 3.5 hours in 10 % EtOH/PBS (95 %)	[19]
5	<b>GaCl(bis(thiosemicarbazone))</b> 	K <sub>2</sub> .2.2., K <sub>2</sub> CO <sub>3</sub> DMSO 40–50 °C, 30 min <i>pH</i> not available	1–8 %	At least 2 hours in crude mixture	[18]
6	<b>GaCl(bis-picolinate)</b> 	K <sub>2</sub> .2.2., K <sub>2</sub> CO <sub>3</sub> H <sub>2</sub> O/MeCN 7/93 80 °C, 30 min <i>pH</i> not available	2 %	Not studied	[15]

Table 1. continued					
Entry	Precursor	Reaction conditions	RCY <sup>[a]</sup>	Stability (RCP) <sup>[b]</sup>	Ref
7	X = OH or Cl <b>GaOH(L)</b>	AcONa/H buffer (pH 5) r.t., 20 min	86%	At least 1 hour in NaOAc pH 5	This work
					
[a] RCY = radiochemical yield; [b] RCP = radiochemical purity.					

chelating agent  $H_3(\text{PCTA-C4})$  (Figure 1) have shown that the Ga(III) center is heptacoordinated, and involves a set of  $N_4O_3$  coordination atoms corresponding to the  $N$ -atoms of the pyclen scaffold and a  $O$ -atom from each of the three acetate subunits. To our knowledge, such extended coordination for Ga(III) complexes has never been reported, even in the case of potentially octadentate chelating agents such as those derived from DOTA.<sup>[22]</sup> In addition to deviating from the hexacoordination trend generally reported for  $Ga^{3+}$ ,<sup>[22–24]</sup> these original Single Crystal X-Ray Diffraction (SCXRD) structural data revealed that the three longest coordination bonds are Ga–N bonds (2.299(4), 2.333(5), and 2.363(5) Å), and furthermore that these bonds are longer than those reported from SCXRD studies of other Ga(III) complexes formed with cyclic chelating agents, which are often shorter than 2.20 Å.<sup>[22,24]</sup> Consequently, we hypothesized that at least one of these particular bonds might be sufficiently labile to be broken and allow coordination of a sufficiently strong ternary ligand, such as a fluoride anion, capable of overcoming the entropic stabilization of the intracyclic coordination formed with the  $N$ -atoms of the pyclen. Unfortunately, attempts to displace this arrangement with a large excess of fluoride (KF) failed to produce a  $Ga^{19}F$  complex (See Supporting Information and Figure S31). This previous result led us to modify the chelating agent structure and to consider PC2A-based chelating agents (Figure 1) speculating that they would remain good candidates for capturing Ga(III) species quite strongly, while the apparent hexadentate denticity would be in favor of coordinating a ternary ligand such as fluoride that would otherwise ensure the electronic neutrality of the resulting complex. The bifunctional chelating agent  $H_2(\text{PC2A-OAE-NCS})$  was therefore proposed featuring a PC2A backbone consisting of a pyclen scaffold for the 12-atom tetrazamacrocyclic cavity closely matching the ionic radius of  $Ga^{3+}$ , complemented by two acetate arms to form a neutral complex with a Ga–X species. Finally,  $H_2(\text{PC2A-OAE-NCS})$  incorporates the  $O$ -acetamido-ethyl (OAE) spacer on the pyridine subunit with a highly reactive terminal isothiocyanate function to enable conjugation to a targeting vector. It should be noted that the *ortho* position of this appendage has proved relevant in keeping the groups present on this subunit outside the first coordination sphere of the gallium.<sup>[20]</sup> Moreover, we assumed that the non-symmetric

structure could confer small differences in nucleophilicity/basicity of the set of donor  $N$ -atoms of pyclen, which could also be favorable to the fulfilment of gallium's electronic demand by a ternary ligand while enabling as well potential fine-tuning structural modulation.

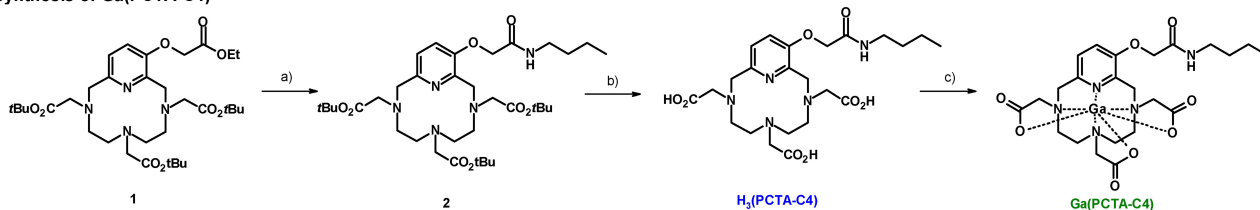
In this study, the PC2A–OAE–NCS derivative denoted  $LH_2$  (Figure 1), which presents a thiourea function to mimic the bioconjugation with a targeted vector, was chosen to explore the radiolabeling process *via*  $Ga-^{18}F$  complexation. The syntheses of the four chelating agents ( $\text{PCTA-C4}$ ,  $\text{PC2A}$ ,  $\text{PC2A-OAE-NCS}$ , and  $LH_2$ ) are described here together with that of the corresponding gallium complex(es). The crystal structures of  $\text{Ga}(\text{PCTA-C4})$  and  $\text{GaF(L)}$  are presented, and the radiofluorination of  $\text{GaOH(L)}$  and  $\text{GaF(L)}$  in water are discussed.

### Synthesis and Characterization of $\text{Ga}(\text{PCTA-C4})$

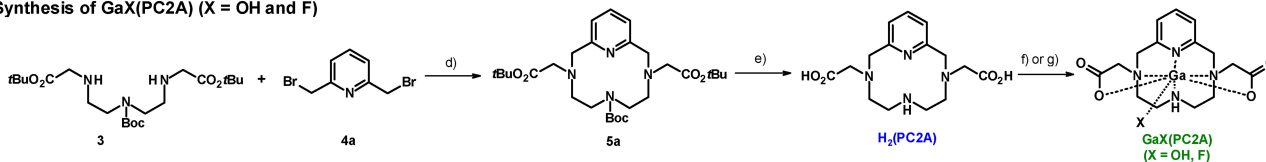
The  $H_3(\text{PCTA-C4})$  chelating agent (Figure 1) was prepared in two steps from the macrocyclic tetra-ester precursor **1** previously described by us.<sup>[25]</sup> The selective aminolysis of the ethyl ester function proceeded gently at room temperature using an excess of *n*-butylamine and led to the corresponding amide **2** in 85% yield (Scheme 1). Cleavage of the *tert*-butyl esters was done by action of a solution of anhydrous hydrogen chloride in diethyl ether and led to the desired  $H_3(\text{PCTA-C4})$  as hydrochloride form(s) recovered by filtration. Further purification by chromatography on reverse-phase (RP18) yielded the product in around 76%. For storage at room temperature and atmospheric pressure, and for its application to the complexation of cationic metal species, the chelating agent was converted to a neutral sodium form at pH 5 and found to be highly stable for at least 6 months, neat in the solid state, and also in aqueous solution ( $^1H$  NMR monitoring, Figure S10).

As expected, the corresponding gallium complex was readily prepared in water, by the action of a slight excess of  $\text{Ga}(\text{NO}_3)_3$  as Ga(III) source and proceeded at room temperature in a few minutes after alkalization to pH 5 with NaOH. The  $\text{Ga}(\text{PCTA-C4})$  complex was isolated after a desalting process by gel filtration chromatography in  $67 \pm 1\%$  ( $n=2$ ) at the 100 mg scale. As previously observed for lanthanide complexes with

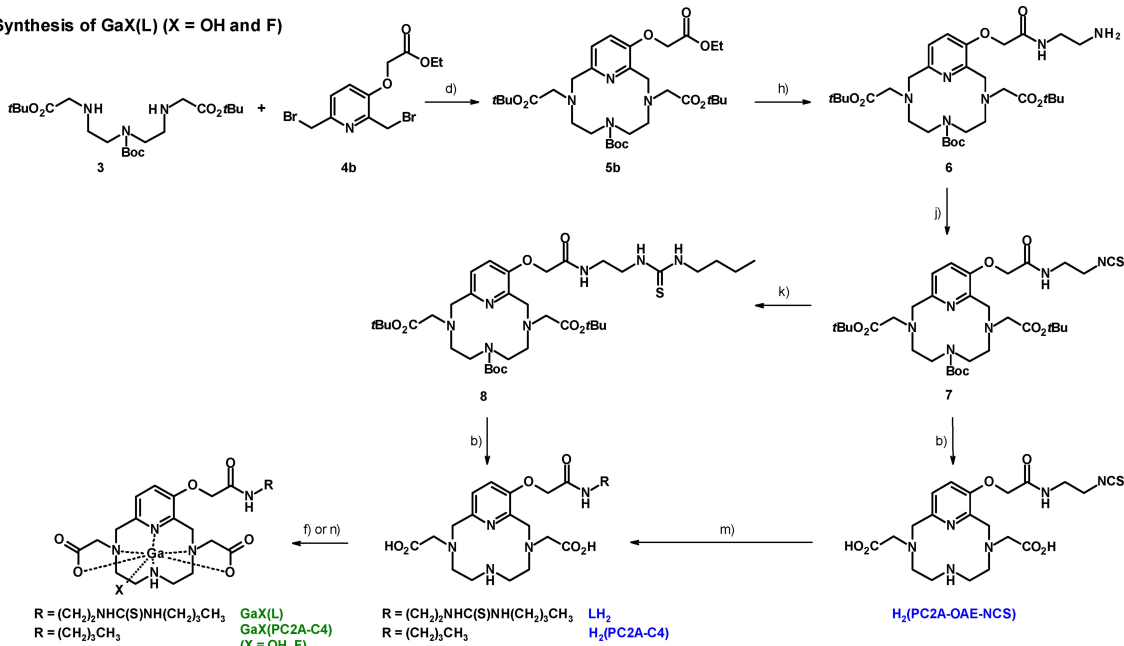
## Synthesis of Ga(PCTA-C4)



## Synthesis of GaX(PC2A) (X = OH and F)



## Synthesis of GaX(L) (X = OH and F)



**Scheme 1.** Synthetic pathway of the pyclen derivatives: a) *n*-butylamine, CH<sub>3</sub>CN, r.t., 24 h; b) HCl<sub>anhr</sub>, Et<sub>2</sub>O, CH<sub>2</sub>Cl<sub>2</sub>, r.t., 7 h; c) Ga(NO<sub>3</sub>)<sub>3</sub>, H<sub>2</sub>O, r.t.; ii) NaOH<sub>aq</sub> to pH 4.9, r.t., 10 min; d) Na<sub>2</sub>CO<sub>3</sub>, CH<sub>3</sub>CN, reflux, 1 h; e) i) 37% HCl<sub>aq</sub>, r.t., 4 h; ii) NaOH<sub>aq</sub> to pH 7.5; f) For X = OH: i) Ga(NO<sub>3</sub>)<sub>3</sub>, H<sub>2</sub>O, r.t.; ii) NaOH<sub>aq</sub> to pH 4.4 or to pH 4.7 for H<sub>2</sub>(PC2A) or LH<sub>2</sub> respectively, r.t., 5 min; g) For X = OH and/or F: Protocol 1: i) Ga(NO<sub>3</sub>)<sub>3</sub>, H<sub>2</sub>O, r.t.; ii) NaOH to pH 5.5, r.t., 5 min; iii) NaF to pH 7.5, r.t., 1.5 day; Protocol 2: i) Na<sub>2</sub>GaF<sub>5</sub>, H<sub>2</sub>O, r.t., 5 min; ii) NaOH<sub>aq</sub> to pH 5.0, r.t.; h) ethylenediamine, r.t., 1 h; j) CCl<sub>4</sub>, DIPEA, CH<sub>2</sub>Cl<sub>2</sub>, r.t., 30 min; k) *n*-butylamine, CH<sub>2</sub>Cl<sub>2</sub>, r.t., 1.5 h; m) For H<sub>2</sub>(PC2A-C4): i) NaOH<sub>aq</sub> to pH 7, H<sub>2</sub>O; ii) *n*-butylamine, r.t., overnight; n) For X = OH and/or F: Protocol 1: i) Ga(NO<sub>3</sub>)<sub>3</sub>, H<sub>2</sub>O, r.t.; ii) NaF to pH 4.4 or to pH 4.0 for LH<sub>2</sub> or H<sub>2</sub>(PC2A-C4) respectively, r.t., 5 min; Protocol 2: i) Na<sub>2</sub>GaF<sub>5</sub>, H<sub>2</sub>O, r.t., 5 min; ii) NaOH<sub>aq</sub> to pH 5.1, r.t.

chelating agents derived from H<sub>3</sub>(PCTA),<sup>[26]</sup> complexation can be monitored by UV-Vis spectroscopy, as it induces a red shift of the ligand-centred  $\pi-\pi^*$  transitions. In the present system, the chelating agent H<sub>3</sub>(PCTA-C4) is characterized by a  $\lambda_{\text{max}}$  of 280 nm, while the corresponding Ga(PCTA-C4) complex shows a  $\lambda_{\text{max}}$  of 288 nm (Figure S30).

The stability of the pure compound in the solid state, or in aqueous solution (pH 4–5), at room temperature and under atmospheric pressure, was monitored by mass spectrometry and <sup>1</sup>H NMR, and was found to be high, with spectra remaining unchanged after 14 months (Figure S28). This exceptional stability may be due to the effective encapsulation of the gallium ion in the macrocyclic cavity of the pyclen skeleton, with the additional protection afforded by the pendant acetate arms. Elemental analysis of the isolated Ga(III) complex,

resulting from Ga(NO<sub>3</sub>)<sub>3</sub> and the hydrochloride salt of H<sub>3</sub>(PCTA-C4), was consistent with the molecular formula [Ga(PCTA-C4)].4H<sub>2</sub>O.NaCl. Nevertheless, based on the results of Bhalla *et al.* for the GaCl(Bn-NODA) chloride complex prepared with Ga(NO<sub>3</sub>)<sub>3</sub> and the pentadentate chelating agent Bn-NODA as its hydrochloride form,<sup>[14]</sup> the molecular formula [GaClNa(PCTA-C4)].4H<sub>2</sub>O could also be proposed. In this second case, based on the widely assumed maximum coordination number of 6 for Ga(III), very generally observed in solid-state structures from X-Ray Diffraction (XRD) data,<sup>[23,27]</sup> one could hypothesize that only two of the three pendant carboxylate arms would be involved in Ga<sup>3+</sup> immobilization, charge neutrality then being ensured by a ternary chloride. In this case, fluorination by anion exchanges CO<sub>2</sub>/F or Cl/F could have been considered. Unfortunately, from Ga(PCTA-C4) com-



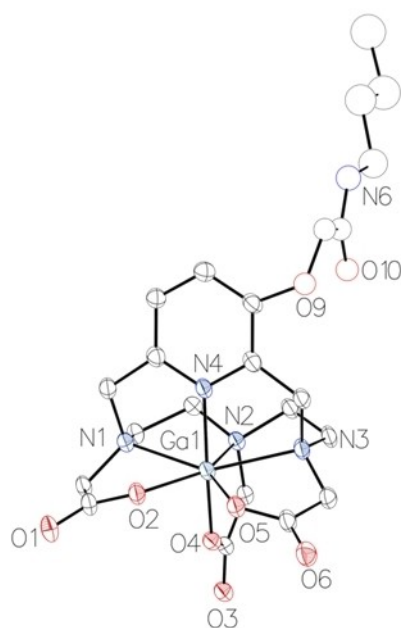


**Figure 2.** ORTEP view of the crystal structure of Ga(PCTA-C4). Thermal ellipsoids are drawn at 10% probability plot. H atoms and other disordered parts are omitted for clarity.

Table 2. Selected bond lengths and angles for Ga(PCTA-C4).	
Bond lengths (Å)	
Ga1–O4 (carboxylate axial)	1.876(3)
Ga1–N4 (pyridine axial)	1.985(2)
Ga1–O2 (carboxylate equatorial)	2.064(4)
Ga1–O5 (carboxylate equatorial)	2.076(4)
Ga1–N3 (amine equatorial)	2.299(4)
Ga1–N1 (amine equatorial)	2.333(5)
Ga1–N2 (amine equatorial)	2.363(5)
Bond angles (°)	
O2–Ga1–O5	72.42(15)
O2–Ga1–N1	71.46(16)
O4–Ga1–O2	93.81(15)
O4–Ga1–O5	90.79(16)
O4–Ga1–N1	94.28(15)
O4–Ga1–N2	79.75(15)
O4–Ga1–N3	100.30(15)
O4–Ga1–N4	164.02(16)
O5–Ga1–N3	72.29(15)
N1–Ga1–N2	73.25(15)
N3–Ga1–N2	74.16(15)
N4–Ga1–O2	96.71(14)
N4–Ga1–O5	103.82(14)
N4–Ga1–N1	77.81(14)
N4–Ga1–N2	84.65(15)
N4–Ga1–N3	78.53(14)

plex, no analytical evidence of fluorination was obtained when attempts were made to displace its coordinative set of atoms with a large excess of fluoride (See Supporting Information).

To consolidate this result, more complete structural data were required and XRD structure determination was considered. Several attempts have been made to obtain crystals by slow evaporation of mixtures from a concentrated aqueous solution of the Ga(III) complex mixed with varying amounts of a miscible organic solvent (MeOH, EtOH, *i*PrOH, AcOEt, CH<sub>3</sub>CN). Mixtures of water with EtOH or with *i*PrOH produced small crystals, and those from the mixture water/*i*PrOH proved to be single crystals of XRD quality. The crystal structure of Ga(PCTA-C4) is shown in Figure 2, selected bond lengths and angles in Table 2. Full crystallographic details can be found in Supporting Information. In this crystal, Ga(III) proved to be heptacoordinated with a distorted pentagonal bipyramid (*D*<sub>5h</sub> geometry) arrangement and a set of donor atoms unequivocally of *N*<sub>4</sub>*O*<sub>3</sub>-type. The pentagonal pseudo-plane formed by the equatorial ligating atoms (N1,N2,N3,O5,O2) is characterized by a Root Mean Squared Distance (*RMSD*), defined as the variation in the distance between these atoms and their best-fit plane, of 0.245 Å. The Ga(III) atom deviates from this plane by a distance of 0.072(2) Å. This definitely ruled out the hypothesis of potential coordination of the ternary chloride anion ligand at the expense of a carboxylate pendant arm and reinforced the need to prepare chelating agent with a PC2A backbone to develop a system suitable for radiofluorination based on the coordination of the pseudo-metallic (Ga<sup>18</sup>F) species. The following preliminary study on the chelating agent H<sub>2</sub>(PC2A) was therefore envisaged to validate this concept.

### Synthesis and Characterization of GaX(PC2A) with X = OH, F

Two procedures for the synthesis of 3,9-PC2A, hereinafter referred to as PC2A (Figure 1), have been reported in the literature.<sup>[28,29]</sup> Both are based on the regioselective di-*N*-functionalization of the macrocyclic precursor **pyclen** and the two pathways gave very different results: 5% (2 steps) for a 5 mg scale and a product contaminated with the regioisomer **3,6-PC2A**,<sup>[29]</sup> or 71% (3 steps) for the gram scale but a process involving large excesses of strong acid and strong base.<sup>[28]</sup> In this work, **PC2A** was synthesized using a different route: as previously used for the other **pyclen** derivatives discussed here, it is based on the assembly of two pre-functionalized synthons (Scheme 1).<sup>[30]</sup>

The triamine **3** was prepared according to slight modifications of previous protocols implemented by us and led to the desired synthon on a scale of a dozen grams with a high yield of 85% for three steps, two of which were one-pot (Scheme S1). The dibromide **4a** was prepared as previously described.<sup>[31]</sup> The two synthons were reacted in refluxing acetonitrile in the presence of Na<sub>2</sub>CO<sub>3</sub> and led to the macrocyclic precursor **5a** isolated in moderate 47% yield after purification. Complete deprotection of the amine and carboxylic acids was then achieved by the action of a concentrated 37% aqueous solution of hydrochloric acid. With such a process, **PC2A** was isolated at

*pH* 5 in 40% (2 steps) after purification (desalting procedure on reverse-phase chromatography) to the scale of 100 mg (Scheme 1).

The complexation step proceeded readily at room temperature, similar to that performed previously for **Ga(PCTA-C4)**, and the **GaOH(PC2A)** complex was isolated in quantitative yield after a desalting process by reverse-phase chromatography at the 150 mg scale. As usual, evidence of complexation is unequivocally obtained by  $^1\text{H}$  NMR with splitting on the spectra very commonly observed. Thus **GaOH(PC2A)** is characterized by a  $^1\text{H}$  NMR spectrum with the methylene attached to the pyridine split into an AB system. More remarkably, a diastereotopic split of the two protons of the methylene adjacent to the secondary amine is also observed, which could indicate a strong coordination of the corresponding *N*-atoms (Figure S32). The synthesis of the **GaF(PC2A)** was initially envisaged from **GaOH(PC2A)** precursor by displacement of the ternary hydroxide ligand using an excess of fluoride. Remarkably, this displacement occurred in water at room temperature. Both  $^{19}\text{F}$  NMR and mass spectrometry analyses validates the  $\text{OH}/^{19}\text{F}$  exchange; however, neither can confirm the completion of this exchange. Indeed, the  $^1\text{H}$  NMR spectra of the two species are very similar (Figures S32 and S35). Furthermore, the isotopic pattern observed in mass spectrometry (electrospray ionization) accounts for the detection of both **GaF(PC2A)** and **GaOH(PC2A)** species, the latter possibly also resulting from hydrolysis of **GaF** species in the ion source. Given the absence of analytical evidence of the purity of the **GaF(PC2A)** complex isolated with this protocol, an alternative protocol was considered with a soluble form of the  $\text{GaF}_3$  reagent commonly assumed to be insoluble in water. To this end, the " $\text{Na}_2\text{GaF}_5$ " reagent was prepared in accordance to the recent patent by Xu *et al.*,<sup>[32]</sup> simply by mixing  $\text{Ga}(\text{NO}_3)_3$  and  $\text{NaF}$  in the stoichiometry ratio 1/5 in water and at the appropriate concentration of  $\sim 5$  mM. This gave a slightly acidic solution of *pH* 4.6, which was then concentrated to give a solid compound of formal formula " $\text{Na}_2\text{GaF}_5 \cdot 3\text{NaNO}_3$ ".

This inorganic mixture was characterized by  $^{19}\text{F}$  NMR,  $^{71}\text{Ga}$  NMR, and FTIR. The  $^{19}\text{F}$  NMR revealed the presence of two fluorinated species:  $\text{NaF}$  with  $\delta \sim -121$  ppm, and a new one with  $\delta \sim -153$  ppm that can be attributed to the resulting expected soluble  $\{\text{GaF}\}$  species. The characterization by  $^{71}\text{Ga}$  NMR showed one large signal centered on  $\delta \sim -41$  ppm, reflecting quite asymmetrical chemical bonds around gallium. Moreover, and surprisingly, concentrated solutions ( $\geq 0.02$  M) in  $\text{D}_2\text{O}$  prepared for  $^{71}\text{Ga}$  NMR analyses gave a turbid liquid phase leading to a white precipitate or demixed liquid phase and characterized by a shift of the large signal to  $\delta \sim -27$  ppm (Figure S25). In contrast, no significant change was observed by  $^{19}\text{F}$  NMR (Figure S23).

Finally, the water-soluble synthetic " $\text{Na}_2\text{GaF}_5 \cdot 3\text{NaNO}_3$ " was characterized by FTIR and displayed a  $\nu$  505  $\text{cm}^{-1}$  in agreement with the few reported data,<sup>[16,33]</sup> which is very distinct from  $\nu$  584  $\text{cm}^{-1}$  obtained for the commercially available  $\text{GaF}_3$  reagent. With these new analytical elements in mind and considering the experimental complexation protocol described in the patent, we performed a second protocol to produce higher

purity batches of **GaF(PC2A)** by employing the initial clear aqueous solution at  $c \sim 5$  mM of " $\text{Na}_2\text{GaF}_5 \cdot 3\text{NaNO}_3$ ". Like the first protocol, the complexation step was conducted in pure water with a stoichiometric amount of " $\text{Na}_2\text{GaF}_5 \cdot 3\text{NaNO}_3$ ", and the MS monitoring revealed a complete conversion in few minutes at room temperature. The resulting  $\text{Ga}(\text{III})$  complex was isolated at *pH* 6 in 98% yield at 150 mg scale after purification (desalting) process. As before,  $^1\text{H}$  NMR,  $^{19}\text{F}$  NMR and mass spectrometry analyses confirmed the complexation of the  $(\text{GaF})^+$  species. The isotopic pattern observed in mass spectrometry again accounts for the detection of the two species **GaF(PC2A)** and **GaOH(PC2A)**; however, in this case, the isotopic pattern is quite distinct than that obtained from the  $\text{OH}/^{19}\text{F}$  exchange protocol, with a deconvolution clearly indicating a ratio in favor of the **GaF** species (Figures S43–S45). Moreover, the signal at  $\delta \sim -152$  ppm in the  $^{19}\text{F}$  NMR spectra confirms the presence of a **GaF** bond (Figures S38–S39). Nevertheless, even if the information is not fundamental at this stage of the investigations, the **GaF** purity of the **GaX(PC2A)** with  $\text{X} = \text{OH}, \text{F}$  batches prepared could not be elucidated. To complete the characterization, the  $^{71}\text{Ga}$  NMR analysis was performed but no signal was observed that is indicative of an absence of symmetry for the  $\text{Ga}(\text{III})$  coordination sphere in solution for this complex.<sup>[34]</sup> This result is not surprising considering the study reported for  $\text{Ga}(\text{DOTA})$  complex,  $\text{DOTA}$  being a 12-membered macrocyclic chelating agent less rigid and more symmetrical than **PC2A**: with such a chelating agent presenting a center of symmetry,  $^{71}\text{Ga}$  NMR gave a very broad signal.<sup>[35]</sup> Additionally,  $^{71}\text{Ga}$  NMR spectroscopy has proven to be a relevant analytical method for verifying the absence of free  $\text{Ga}(\text{III})$  in solution *via* the detection of the  $\text{Ga}(\text{OH})_4^-$  species, which forms as early as *pH* 5 and becomes the predominant species at *pH*  $\geq 6$ .<sup>[36]</sup> Indeed,  $^{71}\text{Ga}$  NMR spectroscopic analyses detected the presence of  $\text{Ga}(\text{OH})_4^-$  species at concentrations below 0.5 mM (See Figure S24). Consequently, the absence of signal in the  $^{71}\text{Ga}$  NMR spectra is also the indication of the absence of free  $\text{Ga}(\text{III})$  in solution. Nevertheless, to ensure that the unsymmetrical  $\text{Ga}$ -complex could not interfere and mask the  $\text{Ga}(\text{OH})_4^-$  signal, increasing additions of  $\text{Ga}(\text{OH})_4^-$  to the deuterated **GaX(PC2A)** solution were made and showed a linear increase in the  $^{71}\text{Ga}$  signal a  $\delta \sim 222$  ppm (Figures S40–S41), allowing us to conclude that no free  $\text{Ga}(\text{III})$  was present in the batches of **GaX(PC2A)**. This validates our simple synthesis/purification process for gallium complexes: it does not require a large excess of gallium and the small excess was removed by precipitation then filtration of the insoluble  $\text{Ga}(\text{OH})_3$  species, which is the major form at *pH* between  $4.5 < \text{pH} < 6$ .<sup>[36]</sup> Finally, the persistent  $^{19}\text{F}$  NMR signal obtained at  $\delta \sim -152$  ppm for **GaF(PC2A)** attests to the high stability in the solid-state at room temperature for at least 13 days, as well as in aqueous solution at  $7.3 < \text{pH} < 7.9$  for at least 2.5 months (Figures S38–S39). The stability of fluorination in aqueous solution at room temperature was also monitored by mass spectrometry and found to be stable over a period of at least 5 weeks (Figure S44). Furthermore, in each case, no trace of decomplexation (free ligand) was detected by  $^1\text{H}$  NMR and/or by mass spectrometry. These preliminary stability data validated the relevance of the **GaF(PC2A)** scaffold



for PET labeling under mild conditions, and encouraged us to pursue the investigations on **LH<sub>2</sub>**, a derivative of the PC2A-based bifunctional chelating agent **PC2A-OAE-NCS**.

### Syntheses and Characterization of GaX(L) and GaX(PC2A-C4) with X = OH, F

**LH<sub>2</sub>** chelating agent is a derivative of the bifunctional chelating agent **H<sub>2</sub>(PC2A-OAE-NCS)** discussed above. **LH<sub>2</sub>** is decorated by a thiourea appendage which serves two main purposes: (i) to mimic the bioconjugation to a biomolecule; (ii) to increase its lipophilicity and its retention on RP18 column for easier fluorination investigation by HPLC. The synthetic route is depicted in Scheme 1 and is analogous to that previously practiced for **H<sub>3</sub>(PCTA-C4)** and **H<sub>2</sub>(PC2A)**: the macrocyclic backbone was formed by assembling the two functionalized synthons **3** and **4b** and led to the macrocyclic tetra-ester precursor **5b**. In this case, the subsequent selective aminolysis of the ethyl ester function took place with ethylenediamine used as solvent resulting in the corresponding amido-amine **6** isolated at the 500 mg scale in 73% yield. The primary amine activation step was then carried out in dichloromethane with thiophosgene in the presence of diisopropylethylamine, and the corresponding isothiocyanate compound **7** was obtained at a gram scale in 80% yield after purification.

Finally, compound **LH<sub>2</sub>** resulted from two subsequent steps: first, conjugation with *n*-butylamine in dichloromethane at room temperature to give the corresponding thiourea **8** in quantitative yield; then, cleavage of the remaining protecting groups by acid treatment with hydrogen chloride. The desired chelating agent **LH<sub>2</sub>** was isolated at pH 6 at the 100 mg scale in 63% yield after purification on reverse-phase chromatography. These two last steps cannot be interchanged. Indeed, from the protected precursor **7**, the new bifunctional chelating agent **H<sub>2</sub>(PC2A-OAE-NCS)** was isolated on the scale of 600 mg with a good yield of around 75% after acid treatment with anhydrous hydrogen chloride. However, during the subsequent *n*-butylamine addition step in water previously alkalized to neutrality with NaOH, the desired **LH<sub>2</sub>** chelating agent was not formed: only side products were recovered including the chelating agent **H<sub>2</sub>(PC2A-C4)** isolated in 31% yield. It results from a transamidation process with *n*-butylamine; the driving force could be the entropically favorable formation of ethylene thiourea which is sparingly soluble in the aqueous reaction medium and was recovered by filtration in 98% yield. Complexations of **LH<sub>2</sub>** with Ga(III) reagents (**Ga(NO<sub>3</sub>)<sub>3</sub>** with NaOH or NaF, **Na<sub>2</sub>GaF<sub>5</sub>**) proceeded smoothly at room temperature, very similarly to those described above for the synthesis of **GaOH(PC2A)** and **GaF(PC2A)**. Complexation of the side product **H<sub>2</sub>(PC2A-C4)** was also considered to prepare the **GaF(PC2A-C4)** complex as an analytical reference for monitoring radiolabeling. Indeed, given the undesired transamidation of the spacer obtained in basic aqueous media in the presence of a strong nucleophile such as *n*-butylamine (see above), such cleavage could also occur under radiolabeling conditions involving **LH<sub>2</sub>** derivatives. The three Ga(III) complexes **GaOH(L)**,

**GaX(L)** and **GaX(PC2A-C4)** with X = OH and/or F were obtained as white solids after desalting procedure performed on cyanopropyl reverse phase chromatography. As discussed above for **GaX(PC2A)** with X = OH and/or F, <sup>1</sup>H NMR, <sup>19</sup>F NMR and mass spectrometry analyses confirmed the complexation of the (GaX)<sup>+</sup> species. <sup>19</sup>F{<sup>1</sup>H} NMR gave a single resonance at δ ~ -150 or -151 ppm corresponding to the Ga-F bond. As before, the <sup>1</sup>H NMR (Figure 3) and <sup>13</sup>C NMR (Figure S48) spectra of the two complexes **GaOH(L)** and **GaX(L)** with X = OH and/or F are very similar and do not allow to assess the GaF purity of the batches of **GaX(L)** with X = OH and/or F prepared. By mass spectrometry, again, the isotopic pattern observed in the *m/z* 660–664 range accounts for the detection of both **GaF(L)** and **GaOH(L)** species, bearing in mind that the GaOH species may also result from hydrolysis in the ion source of the **GaF(L)** species (Figure S50). The same applies for the isotopic pattern observed in the *m/z* 558–562 range for the detection of both **GaF(PC2A-C4)** and **GaOH(PC2A-C4)** species (Figure S61). The FTIR spectra of the two compounds **GaOH(L)** and **GaX(L)** with X = OH and/or F also are quite similar, with only a minor difference in the 600–500 cm<sup>-1</sup> region and a signal at ν 553 cm<sup>-1</sup> that could be characteristic of the Ga-F bond in the batches of **GaX(L)** with X = OH and/or F prepared (Figure 4).<sup>114</sup> In conclusion, and as previously mentioned for the Ga(III) complexes prepared with **H<sub>2</sub>(PC2A)**, the GaF purity of the **GaX(L)** batches with X = OH and/or F could not be assessed by any of these analytical techniques; on the other hand, the purity of the **GaF(L)** compound prepared with soluble **Na<sub>2</sub>GaF<sub>5</sub>** as Ga-F source will be proven by the XRD study envisaged later (*vide supra*). Nevertheless, as previously observed for **GaX(PC2A)** with X = OH and/or F, mass spectrometry monitoring confirmed the stability of fluorination for **GaX(L)** at room temperature in pure aqueous solution, in sodium acetate buffer (5 mM; pH 5.0), or in phosphate-buffered saline (PBS, pH 7.6), for at least 24 h (Figures S65–S67). The stability of fluorination at the solid state (freeze-dried sample) at room temperature for at least 17 days was also evidenced by <sup>19</sup>F NMR monitoring and mass spectrometry (Figure 5, Figures S49 and S69) with a constant ratio of integrations for the signals assigned to NaF vs GaF (δ -121.1, and -149.9 ppm respectively) obtained in <sup>19</sup>F NMR. Furthermore, in the solid state and in solution, the high stability of the Ga(III) complex in such pyclen-based chelating agent was also confirmed as no sign of demetallation (Ga(III) release) was detected by mass spectrometry or <sup>1</sup>H NMR (Figure S47 and Figures S65–S69). Finally, the high stability of **GaF(L)**, in terms of Ga(III) release (absence of free ligand) and persistence of fluorination, was demonstrated by mass spectrometry for at least 4.5 months on a sample left in aqueous solution at room temperature (Figure 5 and Figure S68). Indeed, no change was observed in the isotopic pattern in the *m/z* 660–663 range corresponding to the detection of both **GaF(L)** and **GaOH(L)** species, implying inertia of the fluorinated species to hydrolysis (Figure S68).

In order to gain a more complete description of the coordination geometry of the Ga(III) site, and also to prove the purity of **GaF(L)** as a single species, X-ray crystallographic structure analysis was considered. In this case, attempts to

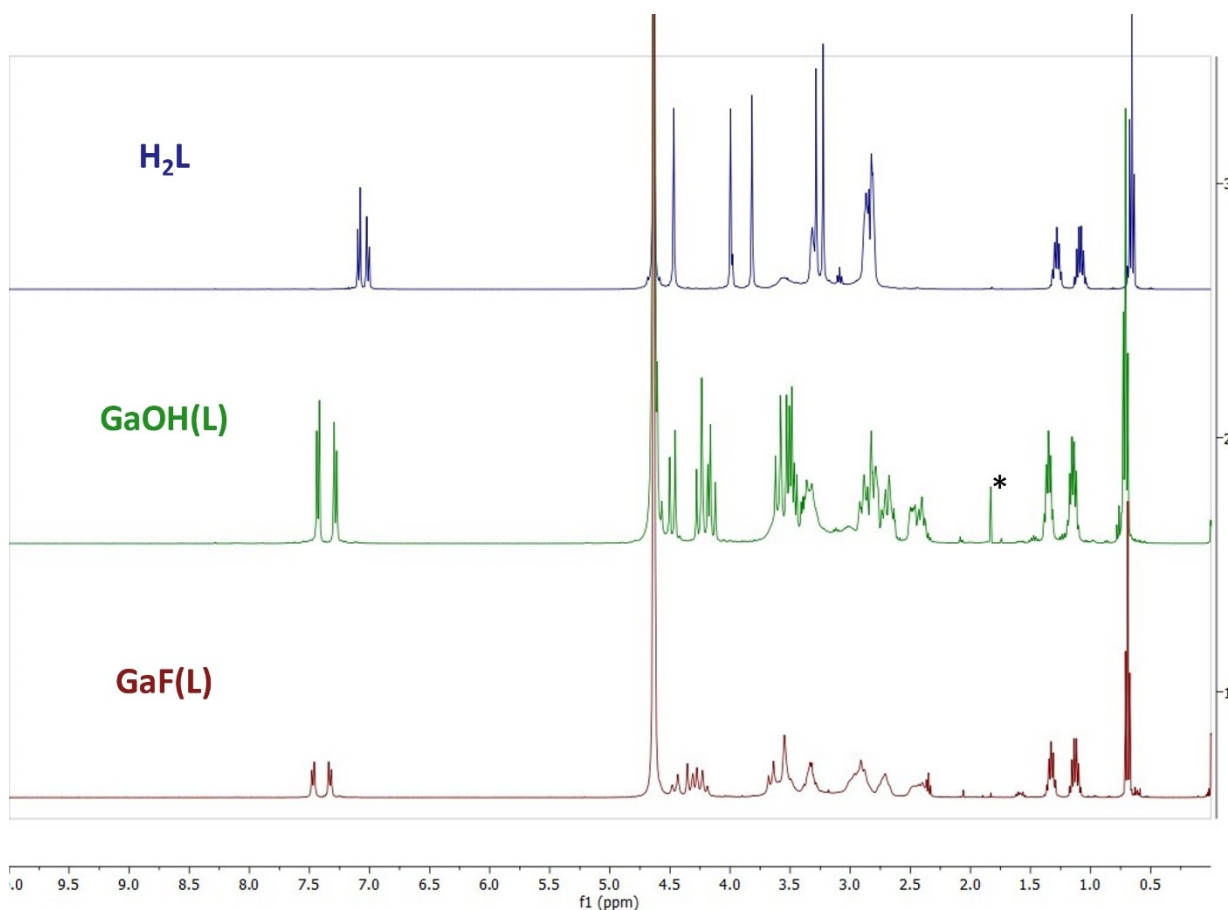


Figure 3.  $^1\text{H}$  NMR spectroscopy of  $\text{LH}_2$ ,  $\text{GaOH(L)}$  and  $\text{GaF(L)}$  in  $\text{D}_2\text{O}$ ; (\* : residual solvent).

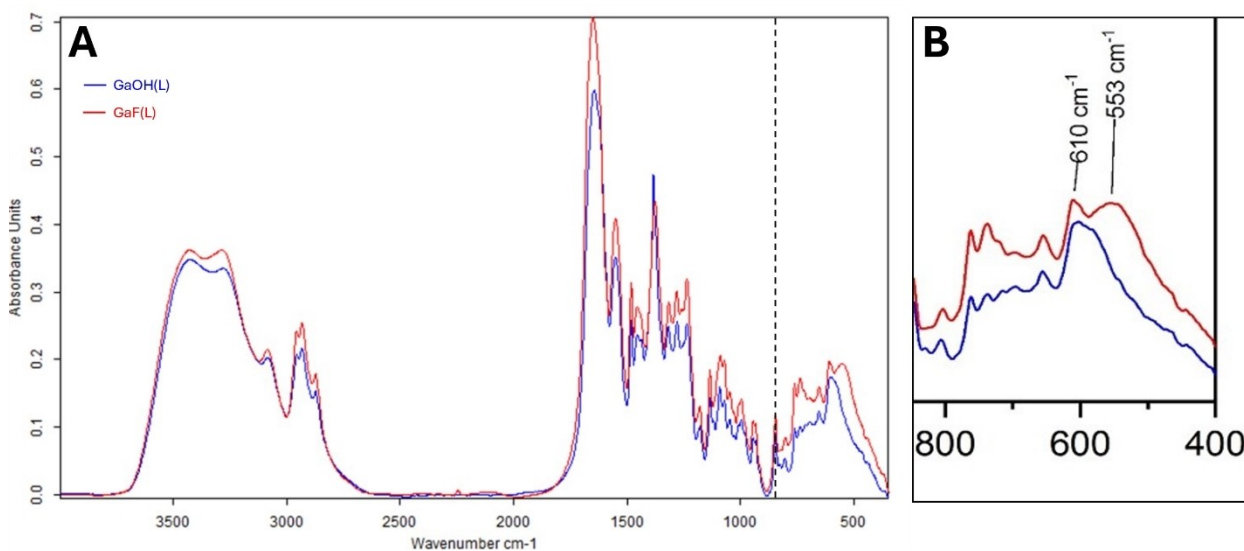
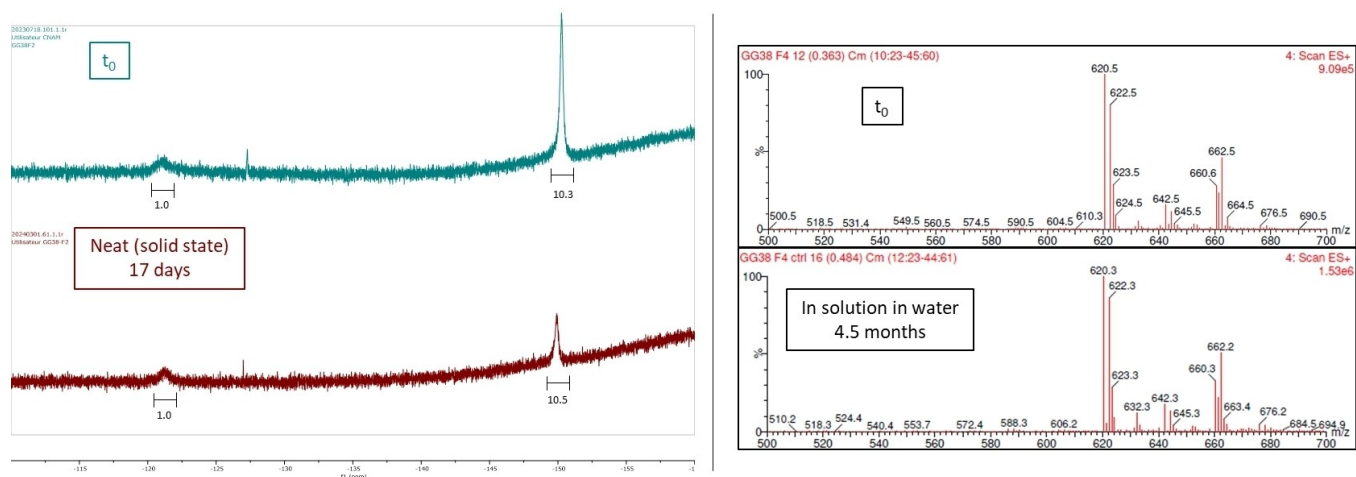


Figure 4. FTIR overlaid spectra of  $\text{GaOH(L)}$  and  $\text{GaF(L)}$  on KBr pellet (64 scans).

obtain crystals by slow evaporation of an aqueous solution of  $\text{GaF(L)}$  in the presence of variable amounts of a miscible organic solvent (MeOH, EtOH or acetonitrile) remained unsuccessful. However, XRD quality single crystals of  $\text{GaF(L)}$  were obtained from a high-throughput crystallization screening by

following the procedure and protocols established for biological macromolecules.<sup>[37]</sup>

The crystallization, XRD data collection and structure resolution can be found in Supporting Information. The crystal



**Figure 5.** Stability of GaF(L) at room temperature: neat in the solid state (lyophilisate) and in solution in water.

structure of GaF(L) is shown in Figure 6, selected bond lengths and bond angles in Table 3.

In this crystal, the unusual heptacoordination of Ga(III) that we had observed on Ga(PCTA-C4) has again been observed and involves a set of  $N_4O_2$  donor atoms complemented by the coordination to a fluoride anion. A pentagonal bipyramid geometry is apparent with the fluoride ligand and the secondary amine *N*-atom positioned at the apical sites. The shortest bond length was found to be 1.815(2) Å, corresponding to Ga–F, which is in full accordance with reported values. The Ga–F bond in GaF(L) is slightly shorter than those found for the ternary complexes GaF(Bn–NODA) and GaF<sub>3</sub>(Me<sub>3</sub>–tacn) formed with macrocyclic chelating agent (1.821(2) Å, and 1.851(3) to 1.881(3) Å respectively), and slightly longer than that found for GaF(dpa–Bn) formed with an acyclic pentadentate chelating agent (1.797(2) Å).<sup>[14–16]</sup> The apical Ga–N2 bond length is of 2.036(4) Å is the second shortest bond of the seven of the set. This reflects the robustness of this coordination, which may

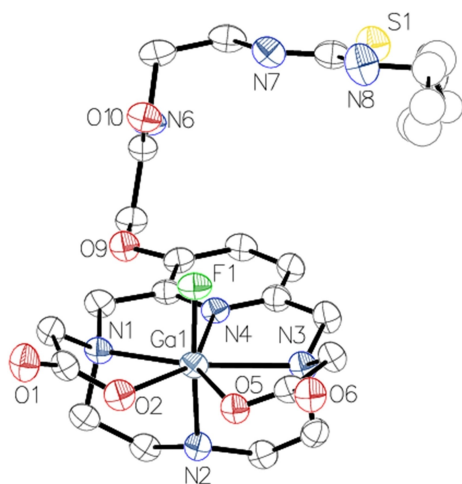


**Figure 6.** ORTEP view of the crystal structure of GaF(L). Thermal ellipsoids are drawn at 10% probability plot. H atoms and other disordered parts are omitted for clarity.

induce an enhanced “protective” envelope of the metal center within the coordination shell provided by the other five *N,O*-heteroatoms. This hypothesis is supported by the *RMSD* of 0.132 Å which characterizes the pseudo-plane formed by the five equatorial ligating atoms (N1,N4,N3,O5,O2), and which therefore turns out to be almost half that found for Ga(PCTA-C4) crystal. Furthermore, the Ga1 atom is located just 0.051 Å above this plane, and the fact that this distance is well below the *RMSD* value indicates that Ga1 is indeed in the equatorial plane. What’s more, the lower ratio of these two parameters, *RMSD* and distance Ga1-pentagonal space, which is 2.6 for GaF(L) versus 3.4 for Ga(PCTA-C4), may augur better protection of the gallium center against various lysis processes. This features confirm that Ga(III) combines well with the PC2A scaffold, which can be considered a good-sized cocoon for Ga(III) species. Furthermore, comparison of the distance between Ga1 and the pentagonal pseudo-plane in the Ga(PCTA-C4) crystal and in the GaF(L) crystal, which is 0.021 Å shorter, or 35% less, suggests that the PC2A scaffold is even more suitable for Ga(III) complexation than the PCTA scaffold. In GaF(L), contrary to that observed previously for Ga(PCTA-C4), the *N*-azine of the pyridine subunit is positioned in the equatorial plan and may induce this exceptional planar conformation formed with the two other *N*-atoms of the tertiary amines of the macrocycle completed by the two *O*-atoms of the two acetate pendant arms. The Ga–N bond lengths range from 2.252 to 2.280 Å, while Ga–O bond lengths are 2.088(3) and 2.106(3) Å in good agreement with values reported for Ga(III) complexes where Ga–N bonds are generally longer than Ga–O bonds.<sup>[22–24]</sup> This study also confirmed the hypothesis that the spacer/bioconjugation site appendage grafted onto the *ortho* position of the pyridine subunit does not participate in the coordination sphere.

Table 3. Selected bond lengths and angles for GaF(L).	
Bond lengths (Å)	
Ga1–F1 (axial)	1.815(2)
Ga1–N2 (amine axial)	2.036(4)
Ga1–O5 (carboxylate equatorial)	2.088(3)
Ga1–O2 (carboxylate equatorial)	2.106(3)
Ga1–N1 (amine equatorial)	2.271(3)
Ga1–N4 (pyridine equatorial)	2.252(3)
Ga1–N3 (amine equatorial)	2.280(3)
Bond angles (°)	
F1–Ga1–O5	91.82(11)
F1–Ga1–O2	90.23(12)
F1–Ga1–N2	171.53(12)
F1–Ga1–N4	85.30(12)
F1–Ga1–N1	95.79(12)
F1–Ga1–N3	93.32(12)
O5–Ga1–O2	71.00(11)
O5–Ga1–N3	72.71(11)
O2–Ga1–N1	72.55(12)
N2–Ga1–O5	94.29(13)
N2–Ga1–O2	97.30(13)
N2–Ga1–N4	86.32(13)
N2–Ga1–N1	82.87(13)
N2–Ga1–N3	82.92(13)
N4–Ga1–N1	72.61(12)
N4–Ga1–N3	72.16(12)

### <sup>18</sup>F Radiolabeling

Three radiolabeling methods were investigated: (i) one pot procedure from the chelating agent, (ii) isotopic exchange <sup>19</sup>F/<sup>18</sup>F, and (iii) anionic exchange OH/<sup>18</sup>F using a preformed gallium complex (Scheme 2). All reactions were conducted at room temperature for 20 min in a reaction volume of 125 μL and involved 6 μmol precursor *i.e.* a concentration *c* 48 mM in gallium chelate or chelating agent. [<sup>18</sup>F]F<sup>−</sup> was produced by cyclotron irradiation, followed by elution from a QMA cartridge using a 0.9% NaCl solution, yielding [<sup>18</sup>F]NaF solutions with an activity of around 10 GBq/mL. At the start of each new radiolabeling campaign, the radiochemical quality of the [<sup>18</sup>F]NaF supplied was checked on the basis of a coordination radiolabeling test with [<sup>18</sup>F]AlF recently optimized in our radiopharmacy (See Supporting Information).<sup>[38]</sup> The radiochemical conversion (RCC) of the assays was determined by analysis of the crude reaction mixtures by HPLC coupled with a radio detector. By analogy with the method practiced for [<sup>18</sup>F]AlF radiolabelings,<sup>[6]</sup> the first protocol tested here was a one-pot procedure involving [<sup>18</sup>F]NaF (50 μL, 271 ± 17 MBq), Ga(NO<sub>3</sub>)<sub>3</sub> (3.0 μmol), and LH<sub>2</sub> ligand (6 μmol), with AcONa/H buffer as additive to complete the reaction volume (Scheme 2, Method 1). Under these conditions (*pH* ≈ 4.2), radiochemical conversion was unsatisfactory (approximately 4%, Figure S74). The other

two protocols investigated in this work use a preformed Ga(III) complex as a precursor to capture [<sup>18</sup>F]F<sup>−</sup> and are based on anion exchange.<sup>[14,16,17]</sup> It is interesting to note that such a strategy has the advantage of being well suited to the development of an <sup>18</sup>F-radiolabeling kit-like method.<sup>[39–41]</sup> In Method 2, GaF(L) was considered for <sup>19</sup>F/<sup>18</sup>F isotopic exchange, while in Method 3, GaOH(L) was used to give rise to OH/<sup>18</sup>F anion exchange. The radiolabeling procedure based on the isotopic exchange <sup>19</sup>F/<sup>18</sup>F was tested (Scheme 2, Method 2) and a very low RCC of about 1% was obtained (Figure S76). While disappointing, this result is in agreement with previous reported results.<sup>[17,19]</sup> The third method was then considered. In Method 3 (Scheme 2), [<sup>18</sup>F]NaF (50 μL, 78 MBq) was added to GaOH(L) (6 mmol) in a *pH* ~ 5 medium consisting of a mixture of water and AcONa/H buffer. The resulting radio-chromatogram is shown in Figure 7. Three radioactive signals were detected. The attributions were made on the basis of the chromatograms obtained with the same analytic method using UV-detection for the Ga<sup>19</sup>F(L) and Ga<sup>19</sup>F(PC2A–C4) analytic references prepared and discussed above (Figure S55 and Figure S64 respectively). Radio-chromatograms of “blank” samples of [<sup>18</sup>F]NaF in mixtures of water and AcONa/H were also taken into account (Figures S71–S72). This led to the following interpretations: the preponderant signal 3/ corresponds to the desired Ga<sup>18</sup>F(L) complex, while the radio-signal 1/ corresponds to free [<sup>18</sup>F]NaF and 2/ to the Ga<sup>18</sup>F(PC2A–C4) complex. Using such a GaOH(L) precursor, a high RCC of 86% was achieved under mild conditions: *pH* 5, at room temperature in 20 min. It is worth noting that the identity of Ga<sup>18</sup>F(PC2A–C4) was confirmed by performing radiolabeling from the previously isolated chelating agent H<sub>2</sub>(PC2A–C4) using the one-pot methodology (Scheme 2, Method 1) (Figure S75). However, at this stage of our knowledge, we have not been able to draw any conclusion as to the origin of Ga<sup>18</sup>F(PC2A–C4) *i.e.* whether it comes from a rearrangement of Ga<sup>18</sup>F(L) during the radiosynthesis (with formation of ethylene thiourea as discussed above) or whether it resulted from the radiolabeling of a batch of

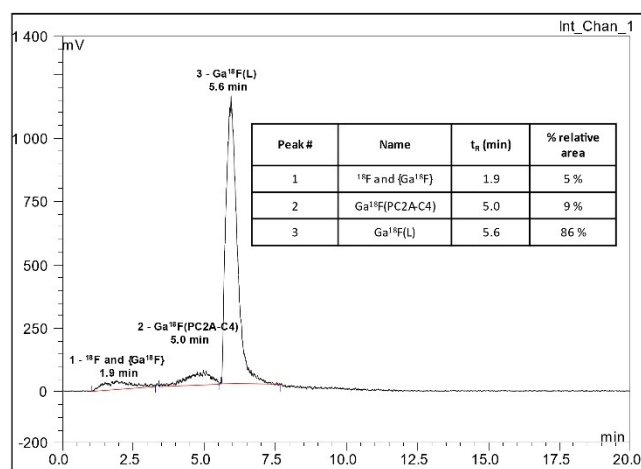
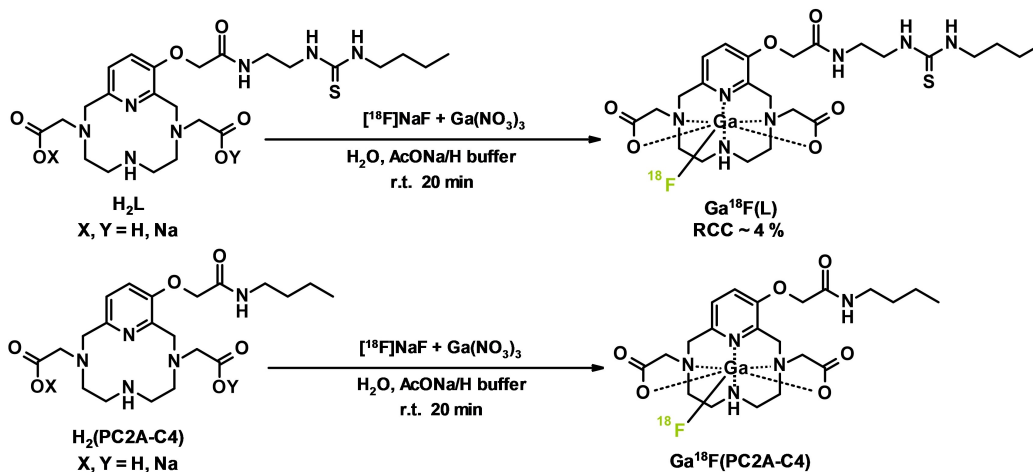


Figure 7. Radiochromatogram by anionic exchange OH/<sup>18</sup>F (Scheme 2, Method 3) of a crude reaction mixture starting from GaOH(L): after 20 minutes at room temperature.



**Method 1: One-pot radiolabeling****Method 2: Radiolabeling via isotopic exchange  $^{19}\text{F}/^{18}\text{F}$** **Method 3: Radiolabeling via anionic exchange  $\text{OH}/^{18}\text{F}$** 

**Scheme 2.** Radiolabeling of  $\text{LH}_2$ ,  $\text{H}_2(\text{PC2A-C4})$ , and  $\text{GaX(L)}$  compounds discussed herein; all assays were carried out with 6  $\mu\text{mol}$  precursor in a reaction volume of 125  $\mu\text{L}$  i.e. a concentration  $c$  48  $\text{mM}$  in gallium chelate or chelating agent.

$\text{GaOH(L)}$  containing  $\text{GaOH(PC2A-C4)}$  as a minor impurity ( $< 5\%$ ).

Further evidence of the successful formation of  $\text{Ga}^{18}\text{F(L)}$  was obtained by LC-MS analysis of the crude reaction mixture after decay of the fluorine-18 (Figures S79-S80). In the light of this study, the  $\text{OH}/^{18}\text{F}$  anionic exchange methodology associated with the preformed  $\text{Ga(III)}$  complex  $\text{GaOH(L)}$  we have developed, has proved very promising, so that the bifunctional chelating agent  $\text{H}_2(\text{PC2A-OAE-NCS})$  we have designed is proving to be a valuable tool for the radiolabeling of sensitive molecules under mild conditions.

**Stability Study of  $\text{Ga}^{18}\text{F(L)}$** 

Given that the presence of unbound  $\{\text{Ga}^{18}\text{F}\}$  and/or free fluoride  $^{18}\text{F}$  species can affect imaging interpretation notably by bone uptake, two aspects of the stability were addressed in this

study: the demetallation *ie* the release of  $\text{Ga}$ , and the defluorination which results from hydrolytic cleavage of the  $\text{Ga}^{18}\text{F}$  bond or any other displacement by a competitive anionic ligand in the medium. As discussed above, high stability in the solid state (freeze-dried sample) and in aqueous media has been demonstrated for the  $\text{Ga}^{19}\text{F(L)}$  complex formed with the non-radioactive natural isotope. The stability of the radioactive complex  $\text{Ga}^{18}\text{F(L)}$  was also investigated. This was done on the crude radiolabeling mixture resulting from Method 3 (Scheme 2) involving acetate buffer ( $c$  36  $\text{mM}$ ), and using radio-HPLC monitoring:  $\text{Ga}^{18}\text{F(L)}$  demonstrated a stability for at least one hour at room temperature (Figure 8).

Our work (Table 1, Entry 7), as a whole, therefore enables us to position our technology in relation to that previously reported by Reid's group (Table 1, Entry 3); indeed, it proceeds in a similar way in pure buffered aqueous medium without the need to add an organic solvent to boost performance as has



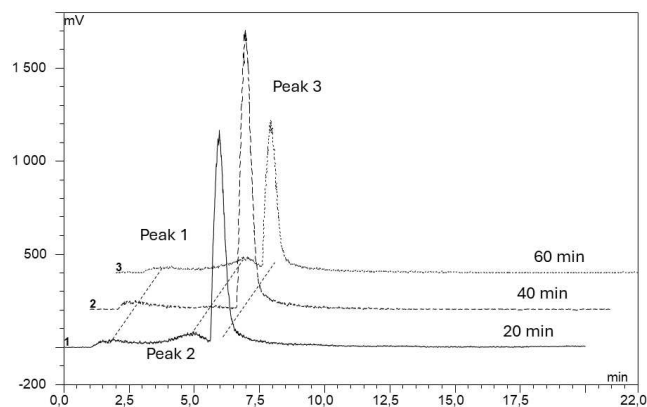


**Figure 8.** Stability at room temperature over the time of  $\text{Ga}^{18}\text{F}(\text{L})$  in the crude reaction mixture resulting from Method 3:  $\text{GaOH}(\text{L})$  *c* 48 mM, in  $\text{H}_2\text{O}$  and  $\text{AcONa}/\text{H}$  buffer (*c* 36 mM), at  $\text{pH} \sim 5$ .

been practiced in other previous work (Table 1, Entries 1–2; 4–6). In our case,  $\text{GaOH}(\text{L})$  was found to give a higher RCC of 86% at room temperature, in 20 min and at a higher  $\text{pH}$  5, compared with the previously reported RCY of 30% after 30 min at  $\text{pH}$  4.<sup>[14]</sup>

## Conclusions

In this study, three cyclen-based derivatives (PCTA, PC2A and L) were investigated as chelating agents for (GaF) species. Based on encouraging results obtained for the  $\text{GaF}(\text{PC2A})$  and  $\text{GaF}(\text{L})$  complexes, in particular their easy synthesis with fast kinetics at room temperature and their high stability under various aqueous media, radiolabeling from  $\text{LH}_2$  and the corresponding preformed  $\text{GaF}(\text{L})$  and  $\text{Ga}(\text{OH})\text{L}$  complexes were envisaged. Three methods were explored to prepare  $\text{Ga}^{18}\text{F}(\text{L})$ . The one based on  $\text{OH}^{18}\text{F}$  anion exchange using  $\text{Ga}(\text{OH})\text{L}$  as precursor was successful, giving an excellent radiochemical conversion (RCC) of 86% at room temperature at  $\text{pH}$  5 without any post-labeling purification step and compared with the radiolabeling by  $(\text{Al}^{18}\text{F})$  coordination generally reported at  $\text{pH}$  4.0 to 4.5.<sup>[7]</sup> Furthermore, the  $\text{Ga}^{18}\text{F}(\text{L})$  radiocomplex proved stable for at least one hour in acetate medium at  $\text{pH}$  5, highlighting the potential of the bifunctional chelating agent  $\text{PC2A-OAE-NCS}$ , and more particularly that of its direct derivative  $\text{GaOH}(\text{PC2A-OAE-NCS})$ , as a valuable prosthetic group for the preparation of targeted PET tracers under mild conditions, as well as for the development of a kit-like  $^{18}\text{F}$ -radiolabeling method for routine clinical use.

In this work, the radiofluorination approach discussed is a prosthetic-type one with a preformed  $\text{GaOH}$  complex to be grafted onto a target molecule (peptide, protein, nanobody). After the radiolabeling step, in a preclinical context, a purification step must be carried out to separate the free  $^{18}\text{F}[\text{F}]^-$  from the radiolabeled probe. As widely reported in the literature, this step could be carried out using commercially available cartridges by solid-phase extraction on alumina or on

reverse-phase sorbent C18, or by size-exclusion chromatography purification step.<sup>[40,42–45]</sup> Additional efforts are underway to consolidate this initial result. Syntheses of a new generation of bifunctional PC2A-based preformed  $\text{GaOH}$  complexes are in progress, with the aim of obtaining similar high RCC at room temperature, but at  $\text{pH}$  closer to the physiological  $\text{pH}$ . This optimization should be supported by a Design of Experiments (DoE) approach recently developed in our group.<sup>[38]</sup> In addition, the new preformed PC2A-based  $\text{GaOH}$  complexes will have to be evaluated for their *in vivo* applicability: *in vitro* stability tests in different media (PBS; human serum) and *in/ex vivo* studies (dynamic PET/CT imaging and biodistribution analysis) on mice to examine in particular *in vivo* stability by quantifying bone retention of the  $\text{Ga}^{18}\text{F}(\text{L})$  radiocomplex.<sup>[11]</sup> Finally, the apparent molar or specific activity  $A_m$  or  $A_s$  of targeted tracers prepared using this technology will also be a crucial element to take into account for future developments and for undertaking preclinical studies on pathological models. These studies represent crucial steps toward harnessing the full potential of these cyclen-based compounds. The results presented here pave the way to overcoming the technological bottleneck which currently limits the potential of radiolabeling of biomolecules sensitive to denaturation induced by acidic media and high temperature, and which remains a major challenge for precision medicine.

## Supporting Information Summary

All experimental data procedure and refinement are detailed in Supporting Information. Parts of these data were also included in a recently filed European patent.<sup>[46]</sup> Moreover, data CCDC 2343109 for compound  $\text{Ga}(\text{PCTA-C4})$ , and CCDC 2361075 for compound  $\text{GaF}(\text{L})$  contain the supplementary crystallographic data for this paper. These data are provided free of charge by the joint Cambridge Crystallographic Data Centre and Fachinformationszentrum Karlsruhe <http://www.ccdc.cam.ac.uk/structures>.

The authors have cited additional references within the Supporting Information.<sup>[47–61]</sup>

## Acknowledgements

The authors would like to thank Dr. Isabelle de Waele (Plateforme de Caractérisation Avancée de l'Institut Chevreuil, LASIRE UMR 8516, Villeneuve d'Ascq (59), France) for scientific discussions and for carrying out some IRFT analyses on KBr pellets. Dr. Louise Breuil (Unité Claude Kellershohn, OPTeN UMR-S 1144, Paris (75), France) is also thanked for her assistance during some radiolabeling assays. Prof Laure Sardamantel is acknowledged for scientific discussions. Prof Franck Denat is thanked for scientific discussions and for providing access to the CHNS elementary analysis service and to the XRD platform of the Institut de Chimie Moléculaire de l'Université de Bourgogne (ICMUB), Dijon (21), France. We would like to thank the staff of the Institut Pasteur crystallography platform (Paris,

France) for screening the crystallizations. We thank the Synchrotron SOLEIL (Saint-Aubin, France) for access to their facility, and the staff of PROXIMA-1 and PROXIMA-2 A for their helpful assistance. The bioprofiling platform supported by the European Regional Development Fund and the Walloon Region (Belgium) is acknowledged. The authors thank the Ligue contre le Cancer (Paris delegation), and the ITMO Cancer of Aviesan (funds administered by Inserm) for their financial support.

### Conflict of Interests

FD, CS, MP have filed a European patent for the radiofluorination methodology presented. The other authors declare no conflict of interest.

### Data Availability Statement

The data that support the findings of this study are available in the supplementary material of this article.

**Keywords:** Fluorine-18 · Gallium · Imaging agent for Positron Emission Tomography (PET) · Macrocyclic N,O ligands · Radiochemistry

- [1] F. M. Bengel, T. Higuchi, M. S. Javadi, R. Lautamäki, *J. Am. Coll. Cardiol.* **2009**, *54*, 1–15.
- [2] V. Valotassiou, J. Malamitsi, J. Papatrifiantayllou, E. Dardiotis, I. Tsougou, D. Psimadas, S. Alexiou, G. Hadjigeorgiou, P. Georgoulas, *Ann. Nucl. Med.* **2018**, *32*, 583–593.
- [3] J. Iking, M. Staniszewska, L. Kessler, J. M. Klose, K. Lücknerath, W. P. Fendler, K. Herrmann, C. Rischpler, *Biomedicines* **2021**, *9*, 212.
- [4] J. P. Pijl, T. C. Kwee, R. H. J. A. Slart, A. W. J. M. Glaudemans, *J. Pers. Med.* **2021**, *11*, 133.
- [5] N. S. Goud, R. K. Joshi, R. D. Bharath, P. Kumar, *Eur. J. Med. Chem.* **2020**, *187*, 111979.
- [6] W. J. McBride, R. M. Sharkey, H. Karacay, C. A. D'Souza, E. A. Rossi, P. Laverman, C.-H. Chang, O. C. Boerman, D. M. Goldenberg, *J. Nucl. Med.* **2009**, *50*, 991–998.
- [7] C. Fersing, A. Bouhlel, C. Cantelli, P. Garrigue, V. Lisowski, B. Guillet, *Molecules* **2019**, *24*, 2866.
- [8] S. J. Archibald, L. Allott, *EJNMMI Radiopharm. Chem.* **2021**, *6*, 30.
- [9] S. Schmitt, E. Moreau, *Coord. Chem. Rev.* **2023**, *480*, 215028.
- [10] F. Cleeren, J. Lecina, E. M. F. Billaud, M. Ahamed, A. Verbruggen, G. M. Bormans, *Bioconjugate Chem.* **2016**, *27*, 790–798.
- [11] L. Russell, J. Martinelli, F. De Rose, S. Reider, M. Herz, M. Schwaiger, W. Weber, L. Tei, C. D'Alessandria, *ChemMedChem* **2020**, *15*, 284–292.
- [12] E. Callegari, J. Martinelli, N. Guidolin, M. Boccalon, Z. Banyai, L. Tei, *Molecules* **2023**, *28*, 3764.
- [13] Y.-R. Luo, *Comprehensive Handbook of Chemical Bond Energies*, CRC Press (Taylor & Francis Group), Boca Raton London New York, **2007**.
- [14] R. Bhalla, W. Levason, S. K. Luthra, G. McRobbie, G. Sanderson, G. Reid, *Chem. Eur. J.* **2015**, *21*, 4688–4694.
- [15] H. Koay, M. B. Haskali, P. D. Roselt, J. M. White, P. S. Donnelly, *Eur. J. Inorg. Chem.* **2020**, *2020*, 3378–3386.
- [16] R. Bhalla, C. Darby, W. Levason, S. K. Luthra, G. McRobbie, G. Reid, G. Sanderson, W. Zhang, *Chem. Sci.* **2014**, *5*, 381–391.
- [17] F. M. Monzittu, I. Khan, W. Levason, S. K. Luthra, G. McRobbie, G. Reid, *Angew. Chem. Int. Ed.* **2018**, *57*, 6658–6661.
- [18] T. K. Venkatachalam, D. H. R. Stimson, R. Bhalla, K. Mardon, P. V. Bernhardt, D. C. Reutens, *J. Label. Compd. Radiopharm.* **2019**, *62*, 321–331.
- [19] D. E. Runacres, V. K. Greenacre, J. M. Dyke, J. Grigg, G. Herbert, W. Levason, G. McRobbie, G. Reid, *Inorg. Chem.* **2023**, *62*, 20844–20857.
- [20] J. Yong-Sang, F. Dioury, V. Meneyrol, I. Ait-Arsa, J.-P. Idoumbin, F. Guibbal, J. Patché, F. Gimié, I. Khantaline, J. Couprie, P. Giraud, S. Benard, C. Ferroud, E. Jestin, O. Meilhac, *Eur. J. Med. Chem.* **2019**, *176*, 129–134.
- [21] C. L. Ferreira, D. T. T. Yapp, D. Mandel, R. K. Gill, E. Boros, M. Q. Wong, P. Jurek, G. E. Kiefer, *Bioconjugate Chem.* **2012**, *23*, 2239–2246.
- [22] V. Kubiček, J. Havlíčková, J. Kotek, G. Tircsó, P. Hermann, É. Tóth, I. Lukeš, *Inorg. Chem.* **2010**, *49*, 10960–10969.
- [23] T. J. Wadas, E. H. Wong, G. R. Weisman, C. J. Anderson, *Chem. Rev.* **2010**, *110*, 2858–2902.
- [24] P. R. W. J. Davey, C. M. Forsyth, B. M. Paterson, *Inorg. Chem.* **2022**, *7*, e202103698.
- [25] M. Devreux, C. Henoumont, F. Dioury, D. Stanicki, S. Boutry, L. Larbanoix, C. Ferroud, R. N. Muller, S. Laurent, *Eur. J. Inorg. Chem.* **2019**, *2019*, 3354–3365.
- [26] J.-M. Siaugue, F. Segat-Dioury, A. Favre-Réguillon, V. Wintgens, C. Madić, J. Foos, A. Guy, *J. Photochem. Photobiol. A* **2003**, *156*, 23–29.
- [27] D. A. Moore, P. E. Fanwick, M. J. Welch, *Inorg. Chem.* **1990**, *29*, 672–676.
- [28] W. D. Kim, D. C. Hrcncir, G. E. Kiefer, A. D. Sherry, *Inorg. Chem.* **1995**, *34*, 2225–2232.
- [29] Z. Garda, E. Molnár, N. Hamon, J. L. Barriada, D. Esteban-Gómez, B. Váradi, V. Nagy, K. Pota, F. K. Kálmán, I. Tóth, N. Lihí, C. Platas-Iglesias, É. Tóth, R. Tripier, G. Tircsó, *Inorg. Chem.* **2021**, *60*, 1133–1148.
- [30] M. Devreux, C. Henoumont, F. Dioury, S. Boutry, O. Vacher, L. V. Elst, M. Port, R. N. Muller, O. Sandre, S. Laurent, *Inorg. Chem.* **2021**, *60*, 3604–3619.
- [31] F. Dioury, C. Ferroud, A. Guy, M. Port, *Tetrahedron* **2009**, *65*, 7573–7579.
- [32] X. Xu (Louisiana State University and Agricultural and Mechanical College), *Antimicrobial Gallium Compounds and Methods*, WO 2019/165425, **2019**.
- [33] E. I. Voit, R. L. Davidovich, A. A. Udovenko, V. B. Logvinova, *Opt. Spectrosc.* **2019**, *127*, 984–990.
- [34] M. I. M. Prata, J. P. André, Z. Kovács, A. I. Takács, G. Tircsó, I. Tóth, C. F. G. C. Geraldés, *J. Inorg. Biochem.* **2017**, *177*, 8–16.
- [35] Q. Zhou, C. Henoumont, L. Vander Elst, S. Laurent, R. N. Muller, *Contrast Media Mol. Imaging* **2011**, *6*, 165–167.
- [36] G. Jackson, M. Byrne, *J. Nucl. Chem.* **1996**, *37*, 379–386.
- [37] P. Weber, C. Pissis, R. Navaza, A. E. Mechaly, F. Saul, P. M. Alzari, A. Haouz, *Molecules* **2019**, *24*, 4451.
- [38] C. San, B. Hosten, N. Vignal, M. Beddek, M. Pillet, L. Sarda-Mantel, M. Port, F. Dioury, *Chem. Eur. J.* **2023**, *29*, e202302745.
- [39] W. J. McBride, C. A. D'Souza, H. Karacay, R. M. Sharkey, D. M. Goldenberg, *Bioconjugate Chem.* **2012**, *23*, 538–547.
- [40] W. Wan, N. Guo, D. Pan, C. Yu, Y. Weng, S. Luo, H. Ding, Y. Xu, L. Wang, L. Lang, Q. Xie, M. Yang, X. Chen, *J. Nucl. Med.* **2013**, *54*, 691–698.
- [41] J. H. Teh, M. Braga, L. Allott, C. Barnes, J. Hernández-Gil, M.-X. Tang, E. O. Aboagye, N. J. Long, *Chem. Commun.* **2021**, *57*, 11677–11680.
- [42] F. Cleeren, J. Lecina, J. Bridoux, N. Devoogdt, T. Tshibangu, C. Xavier, G. Bormans, *Nat. Protoc.* **2018**, *13*, 2330–2347.
- [43] F. Basuli, J. Shi, E. Lindberg, S. Fayn, W. Lee, M. Ho, D. A. Hammoud, R. W. Cheloha, R. E. Swenson, F. E. Escorcia, *Bioconjugate Chem.* **2024**, *35*, 1335–1342.
- [44] S. Wang, Y. Gai, M. Li, H. Fang, G. Xiang, X. Ma, *Bioorg. Med. Chem.* **2022**, *60*, 116687.
- [45] D. Shetty, J. M. Jeong, Y. J. Kim, J. Y. Lee, L. Hoigebazar, Y.-S. Lee, D. S. Lee, J.-K. Chung, *Bioorg. Med. Chem.* **2012**, *20*, 5941–5947.
- [46] F. Dioury, C. San, M. Port, L. Sarda-Mantel (Conservatoire national des arts et métiers), *Fluorine-18 Complex Useful for Positron Emission Tomography*, EP 24 31 5112, **2024**.
- [47] A. Bodor, I. Tóth, I. Banyai, Z. Szabó, G. T. Hefter, *Inorg. Chem.* **2000**, *39*, 2530–2537.
- [48] J.-M. Siaugue, F. Segat-Dioury, I. Sylvestre, A. Favre-Réguillon, J. Foos, C. Madić, A. Guy, *Tetrahedron* **2001**, *57*, 4713–4718.
- [49] K. Ikeda, Y. Yanase, K. Hayashi, Y. Hara-Kudo, G. Tsuji, Y. Demizu, *Bioorg. Med. Chem. Lett.* **2021**, *32*, 127713.
- [50] Chemicalize, Program used for prediction of pKas and speciation curves (December, **2024**; <https://chemicalize.com/>, developed by Chemaxon).
- [51] CrysAlisPro V1.171.38.46, Program for Single Crystal X-ray Diffractometers, Rigaku Oxford Diffraction, **2015**.
- [52] G. M. Sheldrick, *Acta Cryst.* **2015**, *A71*, 3–8.
- [53] G. M. Sheldrick, *Acta Cryst.* **2015**, *C71*, 3–8.
- [54] C. R. Groom, I. J. Bruno, M. P. Lightfoot, S. C. Ward, *Acta Cryst.* **2016**, *B72*, 171–179.
- [55] D. Kratzert, Software: FinalCif; <https://dkratzert.de/finalcif.html2024>, V136.
- [56] A. L. Spek, *Acta Cryst.* **2015**, *C71*, 9–18.

- [57] W. Kabsch, *Acta Cryst.* **2010**, *D66*, 125–132.  
[58] C. Vonrhein, C. Flensburg, P. Keller, R. Fogh, A. Sharff, I. J. Tickle, G. Bricogne, *Acta Cryst.* **2024**, *D80*, 148–158.  
[59] C. Vonrhein, C. Flensburg, P. Keller, A. Sharff, O. Smart, W. Paciorek, T. Womack, G. Bricogne, *Acta Cryst.* **2011**, *D67*, 293–302.  
[60] O. V. Dolomanov, L. J. Bourhis, R. J. Gildea, J. A. K. Howard, H. Puschmann, *J. Appl. Cryst.* **2009**, *42*, 339–341.  
[61] I. J. Tickle, C. Flensburg, P. Keller, W. Paciorek, A. Sharff, C. Vonrhein, G. Bricogne, STARANISO, Program for Determination of Anisotropy of the

Diffraction Limit and Bayesian Estimation of Structure Amplitudes,  
Cambridge, United Kingdom: Global Phasing Ltd, **2018**.

---

Manuscript received: September 20, 2024  
Accepted manuscript online: September 27, 2024  
Version of record online: November 9, 2024